Towards stable kinetics of large metabolic networks: Nonequilibrium potential function approach

Yong-Cong Chen,[1,2] Ruo-Shi Yuan,[1] Ping Ao,[1] Min-Juan Xu,[1] and Xiao-Mei Zhu[1,3,*]

[1]*Key Laboratory of Systems Biomedicine, Ministry of Education, Shanghai Center for Systems Biomedicine, Shanghai Jiao Tong University, Shanghai, 200240, China*

[2]*SmartWin Technology, 67 Tranmere Avenue, Carnegie, VIC 3163, Australia*

[3]*GeneMath, 5525 27th Avenue N.E., Seattle, Washington 98105, USA*

(Received 8 April 2015; revised manuscript received 1 March 2016; published 9 June 2016)

While the biochemistry of metabolism in many organisms is well studied, details of the metabolic dynamics are not fully explored yet. Acquiring adequate *in vivo* kinetic parameters experimentally has always been an obstacle. Unless the parameters of a vast number of enzyme-catalyzed reactions happened to fall into very special ranges, a kinetic model for a large metabolic network would fail to reach a steady state. In this work we show that a stable metabolic network can be systematically established via a biologically motivated regulatory process. The regulation is constructed in terms of a potential landscape description of stochastic and nongradient systems. The constructed process draws enzymatic parameters towards stable metabolism by reducing the change in the Lyapunov function tied to the stochastic fluctuations. Biologically it can be viewed as interplay between the flux balance and the spread of workloads on the network. Our approach allows further constraints such as thermodynamics and optimal efficiency. We choose the central metabolism of *Methylobacterium extorquens* AM1 as a case study to demonstrate the effectiveness of the approach. Growth efficiency on carbon conversion rate versus cell viability and futile cycles is investigated in depth.

DOI: 10.1103/PhysRevE.93.062409

I. INTRODUCTION

Large-scale metabolic networks attract interests from developing diagnostic markers for human diseases to metabolic engineering of bioproducts with economic values [1–4]. In the literature, steady states are often assumed when these systems are analyzed. The existence of reachable steady states on a given metabolic network is apparently consistent with experimental observations [5–9]. On the other hand, steady states for a set of chemical reaction equations are usually difficult to achieve, as many dynamical system theories and previous modeling works have experienced [10–12]. To complicate the issue further, it is impractical to construct a kinetic model purely based on current experimental data due to the unavailability of a large number of parameters [13–17]. Retrofitting to obtain parameters from *in vivo* experiments [11,12] is normally limited to laboratory bacteria.

To avert the difficulty, metabolic analyses mostly rely on static methods that employ stoichiometric matrices and incorporate mass conservation, thermodynamic constraints, and optimization hypotheses [7,18–20]. These approaches would be sufficient if they could adequately reproduce topologies for the underlying networks. Unfortunately, for many systems this is not the case. For example, the flux distribution of central glucose metabolism varies widely across species of bacteria, while the chemical reactions on the metabolism remain conserved [21]. An elementary flux mode method would have yielded the simplest flux mode under the glucose growth condition. Nature, nevertheless, prefers some complex routes for the simple carbon source. Toxic metabolites buildup was suggested as a contributing factor [22]. To verify the hypothesis, a kinetic model is necessary as detailed knowledge of concentration variations becomes essential. Another example that calls for better modeling is the bistability observed in the *Escherichia coli* population after a glucose-gluconeogenic substrate shift [24]. In principle, dynamical aspects of metabolism, such as flux oscillations [25], require proper kinetic models. To date environmental influence on flux distribution remains largely unexplained [21,23].

We investigate the dynamics of a metabolic network by placing metabolism in an adaptive process. The structure of the metabolic network, represented by its entire set of reaction parameters, is assumed to change in time: In our approach, there is a generic "regulatory" dynamics in the parametric space that acts to improve the network stability. The key idea is to employ a dynamical landscape and its associated potential function that can depict the stability of a stochastic network. The existence and construction of the potential function in nongradient systems [26–29] are established via a stochastic dynamical decomposition. The "regulation" draws under the landscape the enzymatic parameters towards the space in which the metabolic network stabilizes. When thermodynamic constraints on chemical reactions are taken into account, the range of the parametric space can be further specified to offer a realistic metabolic model.

The construction of potential functions from general stochastic differential equations in Ref. [26] has been explicitly demonstrated in typical complex nonlinear dynamics, including fixed points [36,37], limit cycles [29,37], and chaotic systems [28]. The stochastic dynamical decomposition leads to a stochastic integration (A-type) which is different from traditional Ito's and Stratonovich's types. The approach adds a unique advantage connecting determinacy and stochasticity through dual roles of the potential functions [27,38]. Experiments confirm that some processes in nature do correspond to the A-type integration [27]. The present work intends to extend the analyses into practically useful computational tools.

*To whom correspondence should be addressed: xiaomeizhu@yahoo.com

Our work is biologically motivated. A living cell differs from an isolated chemical reactor in many ways. Enzymes are constantly synthesized and degraded, activated and inactivated by metabolites and kinases. Metabolites move in and out of the cell in a regulated manner. The concept of regulations is truly generic and everywhere. In this work, we attempt to place the various sources and mechanisms of biological regulations under a unified mathematical description, with a clear goal. The unified regulation aims to identify the regions in the parametric space that can harbor stable steady-state solutions for the metabolic network in question. The stability here refers to the existence of steady-state solutions, and more importantly, the solutions are stable against random noises that are present in any biological system. To achieve the goal, we explicitly introduce stochastic fluctuations at some intermediate steps. At the computational stage, the expressions are simplified with respect to the physiological conditions of a living cell. Finally, in addition to being a tool for metabolic modeling, the mathematics developed in our study may help to clarify other biological regulations that are similar in nature.

II. GENERIC RATE EQUATION

Let us start with the simplest formula for an enzyme-catalyzed reaction, the so-called Michaelis-Menten equation [30],

$$\frac{dy}{dt} = \frac{V_{\max} x}{K_M + x}, \tag{1}$$

where x, y, $V_{\max}$, and K_M are, respectively, the concentrations of the substrate and the product, the maximum reaction rate, and the Michaelis-Menten constant. $V_{\max}$ is determined by both the concentration of the enzyme and its catalytic rate. In an organism, a reaction is often modified via allosteric regulations by additional chemical which binds to the same enzyme and acts to inhibit or activate the enzyme. This can result in effective $V_{\max}$ and K_M that differs from Eq. (1). For example, the presence of a competitive inhibitor with concentration x_I changes the Michaelis-Menten constant to

$$K_M \Rightarrow K_M\left(1 + \frac{x_I}{K_I}\right). \tag{2}$$

Quasisteady states on the intermediate complexes are assumed in Eqs. (1) and (2).

For kinetic modeling of large-scale metabolic networks, there are several obstacles to overcome concerning the enzyme reaction rates. First of all, the modifier(s) to a reaction is not always known. Second, even when the information does exist, the exact form of the reaction rate can be obscured by many unknown parameters. We address the second obstacle by observing that the rate equation of some well-known modification mechanisms, Uni-Uni mechanism, Bi-Uni random mechanism, Bi-Bi ordered mechanism [31], ordered Uni-Bi mechanism, random Bi-Bi mechanism, Ping Pong Bi-Bi mechanism [32] can all be cast into a generic form of enzymatic rate equation. For a typical chemical reaction inside a cell,

$$S_1 + S_2 + \cdots S_m \underset{V_B}{\overset{V_F}{\rightleftharpoons}} P_1 + P_2 + \cdots P_n, \tag{3}$$

where each substrate S_i or product P_i can be the same or different chemicals, the generic rate format representing the reaction can be written as

$$\nu(x_i, y_j) = \frac{V_F \prod_{i=1}^{m} \frac{x_i}{K_i} - V_B \prod_{j=1}^{n} \frac{y_j}{K'_j}}{f_1(V_F, V_B) \prod_{i=1}^{m} \left(1+\frac{x_i}{K_i}\right) + f_2(V_F, V_B) \prod_{j=1}^{n} \left(1+\frac{y_j}{K'_j}\right)}, \tag{4}$$

where x_i and y_j are, respectively, the concentrations of the substrates and the products. In Eq. (4), V_F and V_B are the forward and backward maximum reaction rates. K_i and K'_j are the apparent Michaelis-Menten constants for each substrate and product. f_1 and f_2 are normalization factors given by $f_1(V_F, V_B) = V_F^2/(V_F^2 + V_B^2)$, $f_2(V_F, V_B) = V_B^2/(V_F^2 + V_B^2)$. The generic rate equation is symmetrical in both directions for a reversible reaction and is formally exact under the quasi-steady-state condition. While the decision to employ our simplified rate equation or different forms is a choice of preference [11,12,33], the simplification is convenient for both analytical and computational studies. In the Appendix, an explicit instance of the generic rate equation is derived for the ordered Uni-Bi mechanism.

III. METABOLIC NETWORK

We now consider a metabolic network of N metabolites with their concentrations represented by a $N \times 1$ vector, $x^T = (x_1, x_2, \ldots, x_N)$. The superscript T stands for transverse of a matrix. A set of kinetic questions can be readily written in the form

$$\dot{x} = S\nu(x) + b(x,t) = F(x, V, t), \tag{5}$$

where V denotes a vector in the parameter space covering all the reactions on the network, i.e., V_F and V_B [Eq. (4)] for all reactions, and S is a $(N \times M)$ stoichiometric matrix connecting the reactions to the metabolites. $\nu(x)$ is a $(M \times 1)$ matrix with M being the total number of reactions. Each component of $\nu(x)$ takes the form of Eq. (4). $b(x,t)$ is a $(N \times 1)$ vector representing fluxes in or out of the network. If $b(x,t)$ is not explicit in t, it can be absorbed into the first term by adding virtual reactions to or from a fictitious "external" metabolite. This will be discussed in Sec. V B. Hereafter, we assume $b(x,t) = b(x)$ and $F(x, V, t) = F(x, V)$.

A dynamical system under Eq. (5) is usually unstable: Some metabolites will quickly accumulate and some others deplete as demonstrated by a simple example in Fig. 1. Rather than regarding the selection of reaction parameters as a modeling problem, we need to incorporate both the biological and the mathematical aspects of the model for our study. Here the associated biological question is how a living cell adjusts its parameters and maintains the metabolic stability under fluctuations of concentrations in both metabolites and enzymes (reaction rates). In fact a living cell is assisted by complex biological processes [35]: At a short timescale, metabolites can be transferred in and out of the cell and enzymes are modulated by metabolites. At a longer timescale, enzymes are constantly created and degraded. Note that mass conservation is still satisfied at the coarse-grained level for tissues or colonies.

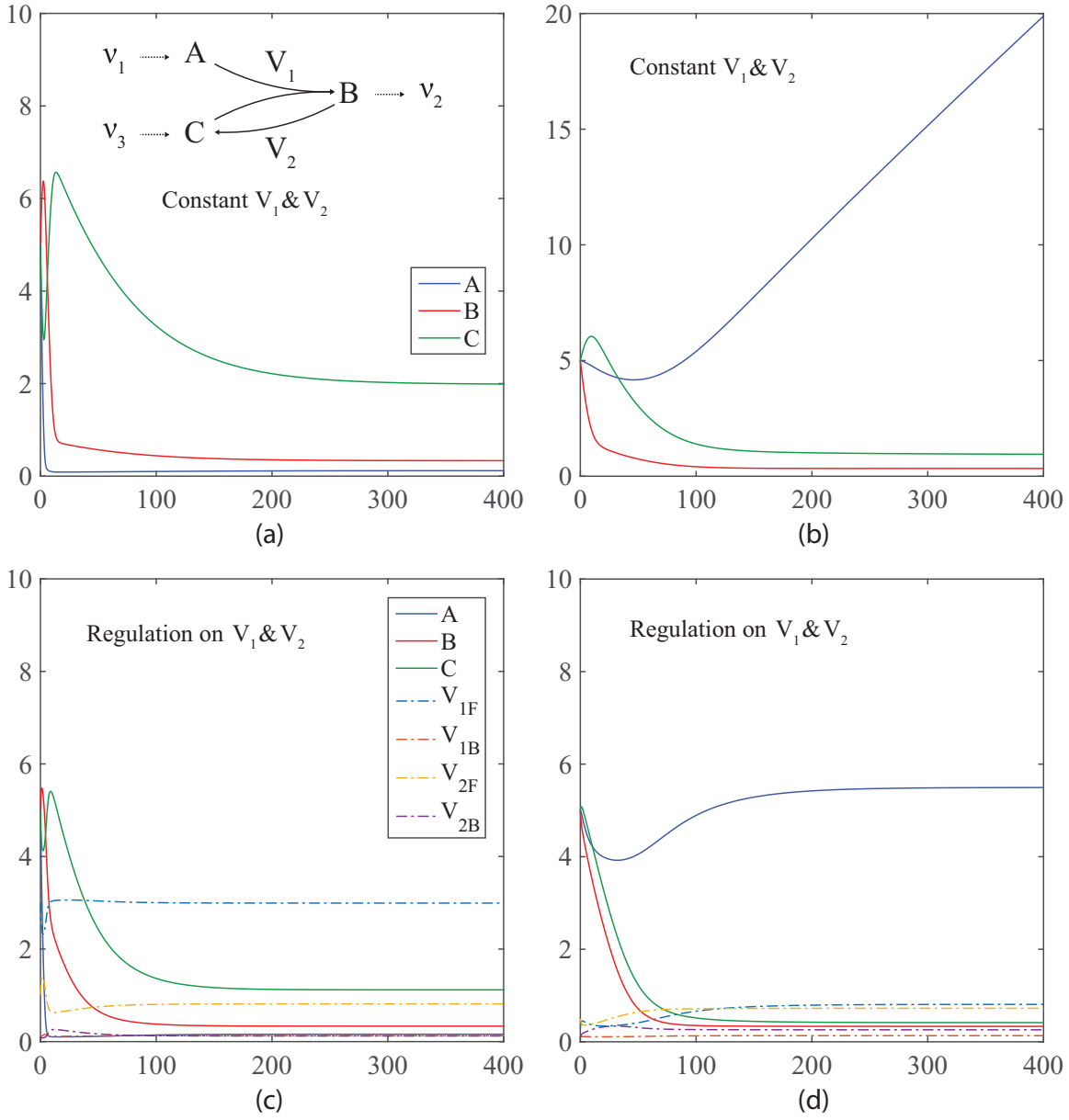

FIG. 1. A simple network of two reactions with input and output fluxes. The network is shown in the inset of (a). When V_{1F}, V_{1B}, V_{2F}, and V_{2B} are constant, the existence of steady-state solution depends on their values. (a) is calculated for $V_{1F} = 3$, $V_{1B} = 0.1$, $V_{2F} = 1$, $V_{2B} = 0.1$ and (b) for $V_{1F} = 0.3$, $V_{1B} = 0.1$, $V_{2F} = 0.5$, $V_{2B} = 0.1$. (c) and (d) are calculated with regulation, starting from the same initial values corresponding to (a) and (b), respectively. The regulation dynamics of Eq. (18) is found to help the system reaching steady states. The solutions are not unique on the network.

Mathematically, the stoichiometric matrix and therefore the form of Eq. (5) remains unaffected. We may regard the parameters in the generic reaction rate Eq. (4), V_F, V_B, K_i, and K'_j as *in vivo* parameters, to be decided by experimental observations and other constraints. We will handle V_F and V_B first.

IV. CONSTRUCTION OF STABLE METABOLIC DYNAMICS

To find out how the enzymatic parameters in Eq. (4) should be regulated in order to achieve stability across the network, we return to Eq. (5) with an addition of random noise ξ, representing stochastic fluctuations over the metabolic network:

$$\dot{x} = F(x,V) + \xi(x,V,t), \tag{6}$$

$$\langle \xi(x,V,t)\xi(x,V,t')^T \rangle = 2D(x,V)\delta(t-t'), \tag{7}$$

where D stands as the diffusion matrix for the noises, and T denotes transpose of a matrix. Note that by stability, we mean that the steady-state solutions can remain stable against random perturbations. The latter are present in any biological system. Thus, having their presence in the construction of the regulation is quite logical.

Although fluctuations exist in any biological system, Eqs. (6) and (7) are not derived explicitly from a microscopic

model, hence questions might arise if the equations are appropriate for the present study. In arriving at the equations, Markov process is explicitly imposed in the time-related part $\delta(t-t')$ in Eq. (7). Such an assumption is widely adopted in stochastic studies related to colloidal particles. In our context, we primarily focus on the metabolic reactions, which are chemical reactions in nature and should be well described by the model. Our choice of the diffusion matrix $D(x,V)$ is not limited to specific forms. In the lack of any specific information, it can be taken as proportional to the concentrations of reactants and reaction velocities. Note that some biological fluctuations might not fall into Markov process and should be further studied. Finally, there is a fine line between stochastic fluctuations and purposeful biological regulations. The latter is precisely the main area of study in this work.

To proceed further, we can use a recently developed method to identify a Lyapunov function for the nongradient system [27]. Following the mathematical analysis developed earlier [26,27], there exists a generalized potential $\phi(x,V)$, a Lyapunov function for Eq. (6) such that

$$[\Sigma(x,V)+\Omega(x,V)]F(x,V) = -\nabla_x \phi(x,V), \tag{8}$$

$$[\Sigma(x,V)+\Omega(x,V)]D(x,V)[\Sigma(x,V)-\Omega(x,V)] = \Sigma(x,V), \tag{9}$$

where $\Sigma(x,V)$ is a nonnegative and symmetric matrix, and $\Omega(x,V)$ is an antisymmetric matrix. Note that both $\Sigma(x,V)$ and $\Omega(x,V)$ are determined by the diffusion matrix D. The precise meaning of the potential ϕ becomes transparent near a stable fixed point, where ϕ can be used to define a Boltzmann-like stationary distribution [36] [cf. below Eq. (15)]. Such a distribution can carry divergence-free probability currents. In the linear case where $F(x,V)$ is a linear function of x, and $D(x,V)$ is constant, the force can be split into two parts, one of which gives rise to a detailed balance with diffusive motions, the other induces cyclic motions on the surface of constant ϕ. A stable metabolic network solution corresponds to a local minimum in the potential $\phi(x,V)$ in our definition. This does not exclude $\phi(x,V)$ from more complex topologies such as a limit cycle when ϕ remains constant in the cycle [29].

We next define a nonnegative cost function $\psi(x,V)$,

$$\psi(x,V) = F(x,V)^T \Sigma(x,V) F(x,V), \tag{10}$$

which is related to the change in the potential for x (under fixed V) in the following way:

For the deterministic part of the dynamics we have

$$\begin{aligned}
&\left.\frac{d\phi(x,V)}{dt}\right|_{V=\text{const}} \\
&= \nabla_x \phi(x,V)\cdot F(x,V) = F(x,V)^T \nabla_x \phi(x,V) \\
&= -F(x,V)^T[\Sigma(x,V)+\Omega(x,V)]F(x,V) \\
&= -F(x,V)^T \Sigma(x,V) F(x,V) \\
&= -\psi(x,V).
\end{aligned} \tag{11}$$

In the above we have used the antisymmetric property of Ω. We further introduce a regulation on V that aims to minimize $\psi(x,V)$ by

$$W(x,V)\frac{dV}{dt} = -\nabla_V \psi(x,V). \tag{12}$$

Here $W(x,V)$ is a matrix whose symmetric part has positive eigenvalues. The form of $W(x,V)$ chosen for our metabolic modeling will be discussed later. We will show below that regulation on V will work toward stabilizing the original network of x.

Let us look at this regulation when the dynamics of the metabolites x and the parameters V are uncoupled. Note that ϕ is in fact a Lyapunov function of the original network when V remains constant [37,38]. On the trajectory of $x(t)$, as a property of Lyapunov function, ϕ monotonically decreases in time. This is indeed confirmed by Eq. (11) as expected. If x is near a steady state, then $d\phi(x,V)/dt \to 0^-$. Therefore, the goal of regulation is to vary V so that $d\phi(x,V)/dt$ can be brought to 0^-. When x is held constant and a dynamics in V is imposed in the form of Eq. (12), the V dynamics suppresses ψ, which in turn reduces the change in ϕ via Eq. (12) when x is allowed to change. In other words, it leads the dynamics in x into a more stable parametric space as a result.

We can illustrate explicitly that a coupled dynamics on x and V is assisted by Eq. (12) to become more stable. Since Σ is symmetric and at least semipositive, minimizing ψ via Eq. (12) moves toward $F(x,V)=0$, and the dynamical system is stable when only V is allowed to vary. When both x and V are allowed to change, the system is not necessarily stable. For the stability, we need to have $d\psi/dt \leqslant 0$ along the trajectory of $x(t)$ and $V(t)$, i.e., to decrease the absolute value of $F(x,V)$. For simplicity we set W in Eq. (12) to be an identity matrix (the result is essentially the same for different W). Using the relationships shown in Eqs. (6) and (8), we have

$$\begin{aligned}
\frac{d\psi}{dt} &= \nabla_V \psi \cdot \frac{dV}{dt} + \nabla_x \psi \cdot \frac{dx}{dt} \\
&= \nabla_V \psi \cdot \frac{dV}{dt} + \nabla_x \psi \cdot (F+\xi) \\
&= \nabla_V \psi \cdot \frac{dV}{dt} + \nabla_x (F^T \Sigma F)\cdot F + \nabla_x \psi \cdot \xi \\
&= \nabla_V \psi \cdot \frac{dV}{dt} + \nabla_x (F^T (\Sigma+\Omega) F)\cdot F + \nabla_x \psi \cdot \xi \\
&= -\nabla_V \psi \cdot \nabla_V \psi - \nabla_x (F^T \nabla_x \phi)\cdot F + \nabla_x \psi \cdot \xi \\
&= -\nabla_V \psi \cdot \nabla_V \psi - F_i F_j \partial_{x_i x_j}\phi \\
&\quad - (\partial_{x_i}\phi)(\partial_{x_j} F_i) F_j + \nabla_x \psi \cdot \xi.
\end{aligned} \tag{13}$$

In the final step of Eq. (13), the first three terms control the deterministic part of $d\psi/dt$. If V is unregulated and constant, the first term is zero. To consolidate the argument, we shall show explicitly that the summation of the second and the third terms is negative near a stable fixed point in the unregulated case. Therefore, the first term, arising from the regulation, contributes to stabilize the network with another negative term. Assuming that x_0 is a fixed point, $F(x_0,V)=0$, then linearize $F(x_0,V) = \tilde{F}(x-x_0)$, $\phi = (x-x_0)^T U (x-x_0)$. Here $\tilde{F}$ and U are constant matrices. Equations (8) and (9) can be written as $(\Sigma+\Omega)\tilde{F} = -U$ and $\tilde{F} = -(D+Q)U$, where $(D+Q) = (\Sigma+\Omega)^{-1}$ [26]. Q and Ω are antisymmetric matrices. The

total contribution of the second and third terms to Eq. (13) is

$$\begin{aligned}
&-F_i F_j \partial_{x_i x_j}\phi - (\partial_{x_i}\phi)(\partial_{x_j} F_i)F_j \\
&= -(x-x_0)^T U(D-Q)U(D+Q)U(x-x_0) \\
&\quad -(x-x_0)^T U(D+Q)U(D+Q)U(x-x_0) \\
&= -2(x-x_0)^T U\,DU\,DU(x-x_0) + 2(x-x_0)^T \\
&\quad \times U\,QU\,QU(x-x_0) - (x-x_0)^T \\
&\quad \times (U\,DU\,QU - U\,QU\,DU)(x-x_0) \\
&= T_1 + T_2 + T_3. \qquad (14)
\end{aligned}$$

Let $DU(x-x_0)=u_1$, $QU(x-x_0)=u_2$, then T_1 and T_2 in Eq. (14) become $T_1=-2u_1^T U u_1$ and $T_2=-2u_2^T U u_2$. Note that Σ and Q are a symmetric and an antisymmetric matrix, respectively. For a stable fixed point, eigenvalues of U are positive. Therefore, both T_1 and T_2 are negative. The third term has no definite sign. But we can calculate the average value of T_3. The steady-state probability distribution is given by [26]

$$\rho_0 = \frac{1}{Z}\exp\left[-\frac{1}{2}(x-x_0)^T U(x-x_0)\right]. \qquad (15)$$

We have

$$\begin{aligned}
\langle T_3\rangle &= \int dx_1 dx_2 \ldots dx_N (x-x_0)^T (U\,DU\,QU - U\,QU\,DU) \\
&\quad \times (x-x_0)\frac{1}{Z}\exp\left[-\frac{1}{2}(x-x_0)^T U(x-x_0)\right] \\
&= \mathrm{tr}[(U^{-1})(U\,DU\,QU - U\,QU\,DU)] \\
&= tr(DU\,QU - QU\,DU) = 0. \qquad (16)
\end{aligned}$$

Thus, for a stable fixed point without regulation, $d\psi/dt < 0$ as expected. The first term in Eq. (13) adds a negative term to $d\psi/dt<0$, to further stabilize the network. It is possible that the contribution from the regulation is sufficient to bring an unstable fixed point back to stable. This is shown in the simple example given below. However, the above analysis relies heavily on the Boltzmann-like distribution, which is only valid near a stable point. Finally, it is worth mentioning that the regulation moves towards $\psi=0$ by lowering ψ, but it does not guarantee to ever reach it.

A further consideration can be made for practical modeling purposes. If x values are known, V and the stable metabolic network may be obtained from Eq. (11). In the generic enzyme reaction rate equation, x/K is invariant. Since the *in vivo* values of the apparent Michaelis-Menten constants of K are mostly unavailable, we can set $x/K=1$ as a starting point. Although from a network point of view the restriction might appear too strong, in realistic biological systems that is usually the case for a large range of metabolite concentrations. Mathematically, if x/K values are set differently, different V_F and V_B are obtained with no qualitative difference.

A. Network stability, a simple example

Before turning to realistic biologic problems of interest, let us use a simple reaction network model to demonstrate explicitly the idea of this work with just two reactions $A+C \xrightarrow{V_1} B$ and $B \xrightarrow{V_2} C$. The two reactions form a simple cycle in which one unit of metabolite A is lost per cycle, similar to a futile cycle in biology. We also add an input and output to the network. The dynamics of the network is given by

$$\begin{aligned}
\frac{d[A]}{dt} &= v_1 - V_1 = f_A, \\
\frac{d[B]}{dt} &= V_1 - V_2 - v_2 = f_B, \\
\frac{d[C]}{dt} &= -V_1 + V_2 - v_3 = f_C,
\end{aligned}$$

with

$$\begin{aligned}
V_1 &= \frac{V_{1F}\frac{[A]}{K_A}\frac{[C]}{K_C} - V_{1B}\frac{[B]}{K_B}}{\frac{V_{1F}^2}{V_{1F}^2+V_{1B}^2}\left(1+\frac{[A]}{K_A}\right)\left(1+\frac{[C]}{K_C}\right) + \frac{V_{1B}^2}{V_{1F}^2+V_{1B}^2}\left(1+\frac{[B]}{K_B}\right)}, \\
V_2 &= \frac{V_{2F}\frac{[B]}{K_B} - V_{2B}\frac{[C]}{K_C}}{\frac{V_{2F}^2}{V_{2F}^2+V_{2B}^2}\left(1+\frac{[B]}{K_B}\right) + \frac{V_{2B}^2}{V_{2F}^2+V_{2B}^2}\left(1+\frac{[C]}{K_C}\right)}. \qquad (17)
\end{aligned}$$

Here $[A]$, $[B]$, and $[C]$ are the concentrations of metabolites A, B, and C. V_{1F}, V_{1B}, V_{2F}, V_{2B}, K_A, K_B, and K_C are the parameters for the forward and backward maximum reaction rates and the apparent Michaelis-Menten constants as defined in Eq. (4). For demonstration purposes we set $v_1=0.2$ to metabolite A, $v_2=0.2[B]/(1+[B])$ from metabolite B, and $v_3=0.1$ to metabolite C, $K_A=K_B=K_C=1$. The choices are arbitrary and they do not change the qualitative behavior of the system. In Figs. 1(a) and 1(b), we show that the stability of the two-reaction network indeed depends on the choice of V_{1F}, V_{1B}, V_{2F}, and V_{2B}. Next, we include a simplified version of the regulatory dynamics Eq. (12). Note that solving Eqs. (8) and (9) for a given diffusion matrix D is not essential for practical purposes because detailed *in vivo* information of D is largely unavailable. Instead, we can choose an approximate Σ to start with. In general, though, we may not arbitrarily choose Σ while treating D as to be determined reversely by Eqs. (8) and (9). In the case of limit cycle Σ approaches zero on the cycle regardless of D [29].

On the given example, we choose Σ and W so that Eq. (12) becomes

$$\begin{aligned}
\frac{dV_{1F}}{dt} &= -V_{1F}\partial_{V_{1F}}\left(\omega_A f_A^2 + \omega_B f_B^2 + \omega_C f_C^2\right), \\
\frac{dV_{1B}}{dt} &= -V_{1B}\partial_{V_{1B}}\left(\omega_A f_A^2 + \omega_B f_B^2 + \omega_C f_C^2\right), \\
\frac{dV_{2F}}{dt} &= -V_{2F}\partial_{V_{2F}}\left(\omega_A f_A^2 + \omega_B f_B^2 + \omega_C f_C^2\right), \\
\frac{dV_{2B}}{dt} &= -V_{2B}\partial_{V_{2B}}\left(\omega_A f_A^2 + \omega_B f_B^2 + \omega_C f_C^2\right), \qquad (18)
\end{aligned}$$

with f_A, f_B, f_C given by Eq. (17), and $\omega_A = 1/\sqrt{([A][C]V_{1F}/K_A K_C)^2 + ([B]V_{1B}/K_B)^2}$, $\omega_B=\omega_C = 1/(\sqrt{([A][C]V_{1F}/K_A K_C)^2 + ([B]V_{1B}/K_B)^2} + \sqrt{([B]V_{2F}/K_B)^2 + ([C]V_{2B}/K_C)^2})$. The matrix W is assumed to be diagonal. At the limit of small Ω, Eq. (9) implies that Σ scales with the inverse of D. The diffusion matrix D in turn scales with the reaction rates. This is the reason to choose the above ω_A, ω_B, and ω_C. We can further set $[A]/K_A=[B]/K_B=[C]/K_C=1$ in their expressions. With the inclusion of the added regulation, Eqs. (5) and (12) are

then solved simultaneously. We see that in Fig. 1(d) when the initial parameters are chosen to be the same as in Fig. 1(b), the network eventually stabilizes, in contrast to what it does in Fig. 1(b).

Given the simple example, we now briefly discuss its possible connections to realistic biological regulations. The regulation of Eqs. (10) and (12) minimizes a cost function that is essentially the multiplication of the rate of change $F =$ synthesis $-$ utilization for each metabolite and Σ. The minimization of F is nothing but product inhibition and substrate activation, as is often encountered in organisms. For example, elevated blood sugar level in a person triggers the enzyme transcription of glucokinase and fructose 6-phosphate in the liver [30]. The dependence of Σ is subtler. The increase on the diffusion matrix D is better for reactions to be evenly spread and to avoid near-zero reaction rates. This feature might have an implication in the understanding of evolution: Are the reaction topologies of different species such as those in Ref. [21] evolved along this direction?

Note that in the above construction the fluctuations-related D only plays an auxiliary role and can be set to zero at the end if only the stability at the deterministic level is concerned. While the construction of the regulation is formal and analytically shown to be effective towards stability, the approximation used later in this paper may require further validations in their own context. We need to handle the fluctuations more realistically if we wish to explore the relationship between the mathematically constructed regulation and the biological ones found in cells. The latter can be complicated by both chemical reactions [39] and biological processes involved [40].

V. LARGE-SCALE METABOLIC MODELING

Let us consider how the regulation process can be applied to the forward and backward maximum reaction rates V_F, V_B for metabolic modeling. We would like to find a simplified version of Eqs. (11) and (12) that is both computationally straightforward and biochemically transparent. In general, we expect the diffusion matrix D to scale with the magnitude of the fluxes, i.e., $D \sim F(x,V) \sim (x/K)V_F$ [or $(x/K)V_B$], representing the level of an intrinsic stochastic process [39]. As a result of Eqs. (8) and (9), Σ (and Ω) should scale inversely with D. We further simplify the cost function ψ by taking Ω matrix diagonal for each V_F (or V_B), i.e., a weighted square summation of the related fluxes. The weight should scale with the inverse of metabolite concentrations. Since the dominant part of metabolism is centered around the usage of organic carbons, we simplify the requirement by scaling the weight with the carbon numbers in the chemical formulas; for example, CH_3COOH has a carbon number $=$ 2. The use of carbon number accounts for the stoichiometric relation that a larger compound (with a high carbon number) is synthesized from smaller ones, hence is less abundant in a cell. It is also due to the majority of metabolic reactions being centered around the carbon routes. Moreover, we let $W(x,V)$ to scale as $1/V_F^2$ (or $1/V_B^2$) to counter balance the factor $1/V_F$ (or $1/V_B$) in ψ. This sets a preference to smaller but positive (forward and backward) maximum reaction rates over large ones. In addition, the nonlinear factors before and after the partial differentiation ∂_{v_k} ensures that the solutions fall into small but positive v_k. Finally, we assume that the cost function is evaluated at the physiological values of the ratios $\{x_i/K_i, y_j/K'_j\}$ as appear in Eq. (4). The ratios are either taken from experiments or set to 1. This is based on observations that under normal physiological conditions the reactions in a cell are catalyzed by enzymes that are most effective when the concentrations match the affinities of the underlying enzymes [30].

To summarize the above simplifications in terms of mathematics, we have

$$\tau \frac{dV_k}{dt} = -V_k^2 \partial_{V_k}\left[\left(\frac{1}{V_k N_k}\right)\sum_n (1+c_n)F_n^2(x,V)\right] \qquad V_k \in \{V_F, V_B\}. \tag{19}$$

Here τ is a characteristic timescale for the regulation process, the summation is over the N_k number of metabolites affected by V_k, and c_n is the carbon number of the nth metabolite. Note that any flux balance solution $F(x,V) = 0$ is also a solution to Eq. (19), therefore Eq. (19) can be considered as an enhanced flux balance analysis that attempts to exclude unstable solutions. The overall flow diagram of the modeling procedure is presented in Fig. 2.

A. Thermodynamic constraints

We now revisit Eq. (4) and examine closely the impact of the laws of thermodynamics on a metabolic network. The balance of a chemical reaction is governed by the difference in the apparent Gibbs free energy between the products and reactants, which in turn determines an equilibrium constant $K_{\rm eq}$ for each reaction. Therefore,

$$\frac{V_F \prod_{j=1}^n K'_j}{V_B \prod_{i=1}^m K_i} = K_{\rm eq} \propto \exp\left(-\frac{\Delta G}{RT}\right). \tag{20}$$

Since we do not require Eq. (4) to be an elementary reaction our $K_{\rm eq}$ is not always dimensionless. ΔG may be considered as the one taken from the rate-deciding step in the apparent chemical reaction when it involves several stepwise reactions. A reaction is irreversible if the drop in free energy is sufficiently large. Equation (20) holds under quasistationary states. If we assume most of the reactions are operated under that condition, then for each set of $\{V_F, V_B\}$, Eq. (20) provides a set of optimization conditions for the apparent Michaelis-Menten constants $\{K, K'\}$. In real metabolism, the changes in their values can be the results of inhibition or activation by any third-party metabolites, e.g., via Eq. (2). Note that the invariance of Eq. (4) under $\{x_i/K_i\}$, $\{y_j/K'_j\}$ implies that if the ratios are kept constant, the solutions obtained for $\{V_F, V_B\}$ remain unaffected.

Our operational process for the optimization is as follows. We start with an initial set of $\{x_{0i}/K_{0i}\}$, $\{y_{0j}/K'_{0j}\}$, then optimize K and K' for the best fit to Eq. (20) while keeping the ratios of $\{x/K\}$ and $\{y/K'\}$ fixed. In practice, we use a cost function,

$$\sum_r \left\{\left[\frac{V_F \prod_{j=1}^n K'_{0j}/y_{0j}}{V_B \prod_{i=1}^m K_{0i}/x_{0i}}\right]\cdot\left[\frac{\prod_{j=1}^n y_j}{\prod_{i=1}^m x_i}\right] - K_{\rm eq}\right\}^2, \tag{21}$$

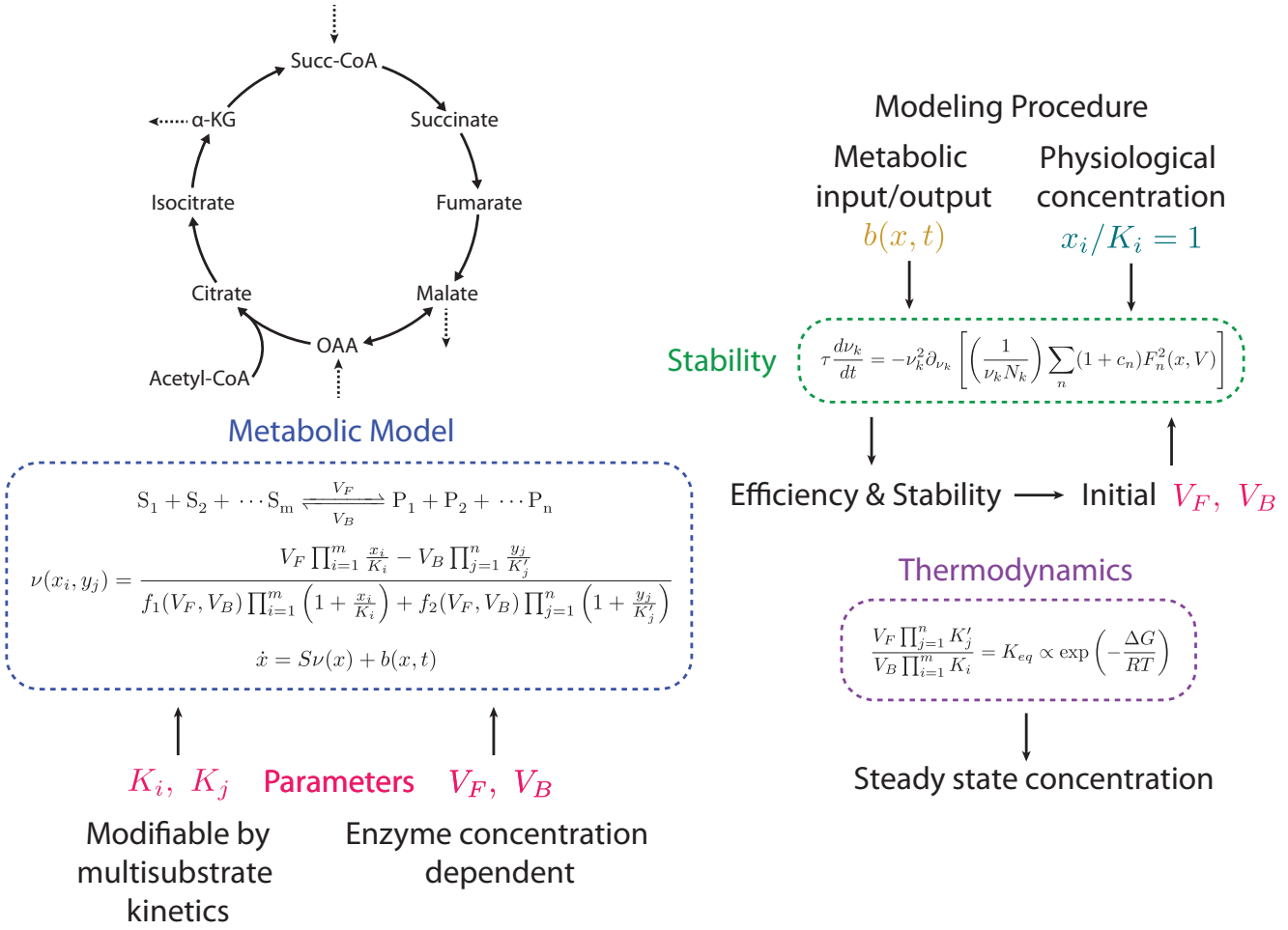

FIG. 2. A summary of the kinetic modeling method employed in the present work. The *in vivo* forward and backward maximum reaction rate V_F, V_B and apparent Michaelis-Menten constants are determined by stability, thermodynamics constraints, and experimental data. Some biological information on the metabolic input or output is required for the metabolite exchanges between the network in the model and the rest of the cell. The exchanges are treated as reactions with an external pool and the maximum reaction rates to be determined in the same manner as that for the normal V_F, V_B via Eq. (19). When initial values of V_F, V_B are smaller, the stable states of the network obtained are more efficient in growth (via carbon conversion rate) but with larger relaxation times. The experimental measured efficiency may be used to pick the most appropriate solution. Without adequate knowledge of *in vivo* enzyme kinetics, steady-state metabolite concentrations are assumed to be on the order of Michaelis-Menten constants, and this assumption is used in Eq. (19). Such an approach can be adjusted when further experimental data are available. In our model, thermodynamic constraints are imposed, independent of the stability requirement, to determine the steady-state metabolite concentrations and the *in vivo* apparent Michaelis-Menten constants.

to determine the optimized concentrations. K and K' is then obtained from $\{x/K\}$ and $\{y/K'\}$ ratio by $\{x/K = x_{0i}/K_{0i}\}$ and $\{y/K' = y_{0i}/K'_{0i}\}$. The summation r runs over all the reactions.

B. Boundary conditions

When only a subset of the complete metabolic reactions in a cell is selected for study, we need to deal with the fluxes between the selected part and the rest of the cell as well as the cellular environment. We employ three types of couplings to model the external interactions in Eq. (5). The first type is to allow a metabolite such as CO_2 or phosphate to maintain a constant concentration. This applies when the metabolite is involved in a large number of reactions, or can transfer in and out of a cell freely or is buffered by other mechanisms. The second type is for certain pair of metabolites, usually coenzymes, e.g., adenosine triphosphate (ATP) and adenosine diphosphate (ADP), where metabolites in the pair always appear on different sides of reactions in which they participate. As a result, the pair's total concentration remains conserved on the network. We handle this type by adding a virtual recycling reaction for each pair to emulate the boundary flow. A third and the most common type of boundary conditions concerns nutrient intakes and biomass productions by the network. They are again handled by fictitious reactions to and from an "external" metabolite, which represents adjustable exchanges between these metabolites and the part of metabolism not included in the model.

C. Initial values

The systematic approach proposed in this paper is intended for a large metabolic network without sufficient parametric

details. In the absence of reliable experimental data, we can set some zeroth-order initial values as the starting point. The model can be improved over time when more accurate values are obtained. In the zeroth order and when no further information is available, the initial concentration of a metabolite is set to 1 mM. Similarly, the initial apparent Michaelis-Menten constants K_i and K'_j of Eq. (4) are set to the respective initial concentrations of the substrates and products involved; i.e., $x_i/K_i = x_j/K'_j = 1$. The thermodynamic equilibrium constants $K_{\rm eq}$ are set to 1 for all reactions that are known to be reversible under the physiological condition in question. We have experimented different choices of initial values V_F and V_B and found that the final flux distribution is only sensitive to the overall scale of the initial values. The regulation process starts with small initial V_F and V_B for all reactions, Eq. (19) works V_F and V_B up and settles into a steady state. This process is similar to switch on a cell from constitutively inactivate enzymes for better metabolism efficiency. When further biological information is available, the choice of V_F and V_B can be changed to represent either a constitutively inactive enzyme (small initial value) or an active enzyme (large initial value) on an individual basis. The above zeroth-order approximation is used in our model study below.

D. Relaxation time

As an application, we show that the dynamical model can be used to estimate dynamical properties of a network. One of them is the relaxation time when deviated metabolic concentrations return to a steady state. Given a set of metabolite outputs from the network (based on the growth rate obtained experimentally), we usually can obtain a range of steady-state solutions. This is done by starting from different sets of initial reaction rates and letting them evolve under Eq. (19). To evaluate the stability of a solution, we can estimate the "relaxation time" reacting to small fluctuations from a given steady state. Biologically shorter relaxation time corresponds to faster response and adaptation to environmental changes. To quantify the analysis, we can linearize Eq. (5) at a steady state to obtain the eigenvalues λ_i of the dynamics near the solution. We define the average or typical response time as

$$\frac{1}{N}\left(\sum_i \frac{1}{\lambda_i}\right), \tag{22}$$

where N is the number of nonzero eigenvalues. Zero ones are excluded from the calculation as they correspond to redundant degrees of freedom in the linearized equations. The number of nonzero values is determined by the rank of the stoichiometric matrix S in Eq. (5). The stability of a solution is justified when there is no eigenvalue with negative real part.

VI. APPLICATION TO *METHYLOBACTERIUM EXTORQUENS* AM1

We have successfully applied our methodology to the central metabolism of *Methylobacterium extorquens* AM1, a methylotrophic and environmental important bacterium that has been extensively studied over the past two decades. In particular, the flux distributions were carefully studied [41]. *Methylobacterium extorquens* AM1 grows on both single and multiple carbon unit compounds. The central metabolism has many well-known metabolic cycles, they adjust in different conditions by changing expressions of relevant enzymes. The metabolic pathways necessary for the growth under methylotrophic conditions are included in our study. It covers formaldehyde metabolism, serine cycle, citric acid cycle, pentose phosphate pathway, poly-hydroxybutyrate (PHB) synthesis, glyoxylate regeneration cycle, gluconeogenesis, serine biosynthesis, and finally electron respiratory chain. The metabolic network used in this work is taken from a previous work [42]. See Supplemental Material for additional information [43]. A summary of the metabolic pathways and the calculated fluxes are depicted in Fig. 3. The results in Fig. 3(a) quantitatively agree across all cycles to that presented in Ref. [42], the latter were constructed from experimentally available data. Figure 4 presents selected real-time plots of concentrations returning to the steady state after a perturbation. Especially, it illustrates a rapid detoxification of formaldehyde in the cell.

Efficiency versus viability

We can explore, as a biological application, the efficiency of growth versus the viability of a cell for *M. extorquens* AM1. In our numerical calculation, the target biomass production and the type of nutrient intake are set first. Starting with small initial V_F and V_B for all reactions the regulation process, Eq. (19), works the way upwards until V_F and V_B are settled into a steady state. Varying the initial values allows us to obtain a range of solutions and compare them to experiments. Larger initial V_F and V_B lead to larger fluxes across the network with lower carbon efficiency (measured by the nutrient intake). The flux topologies remain qualitatively similar. Hence, certain amount of energy appears wasted in some apparent futile cycles. But, as shown in Fig. 3, the lower efficiency solution has a faster relaxation time hence is more stable against random fluctuations. Furthermore, the increase in the futile fluxes at the expense of carbon efficiency smoothes the relative spread of steady-state metabolic concentrations. The spread is an unavoidable consequence of the thermodynamics constraints. Biologically, extreme metabolite concentrations cause fatality as they put severe burdens on osmotic pressure, maintenance, and cellular transport.

The experimental data in Ref. [42] support the less efficient solution shown in Fig. 3. The result indicates that the bacteria do not go with the most efficient metabolism. Instead, they choose to settle into a growth rate that, under the physiological condition, has the optimal balance between efficiency and viability. Finally, the better viability arises from the futile cycles in metabolism for the reasons explained above.

VII. CONCLUSION

To summarize the work, a regulatory dynamics for enzymatic parameters on a large-scale metabolic network has been proposed. It is constructed to draw a vast number of parameters into the phase spaces that stabilize the network. Under a stabilized kinetic metabolic model, thermodynamical constraints, the efficiency of growth and the viability of

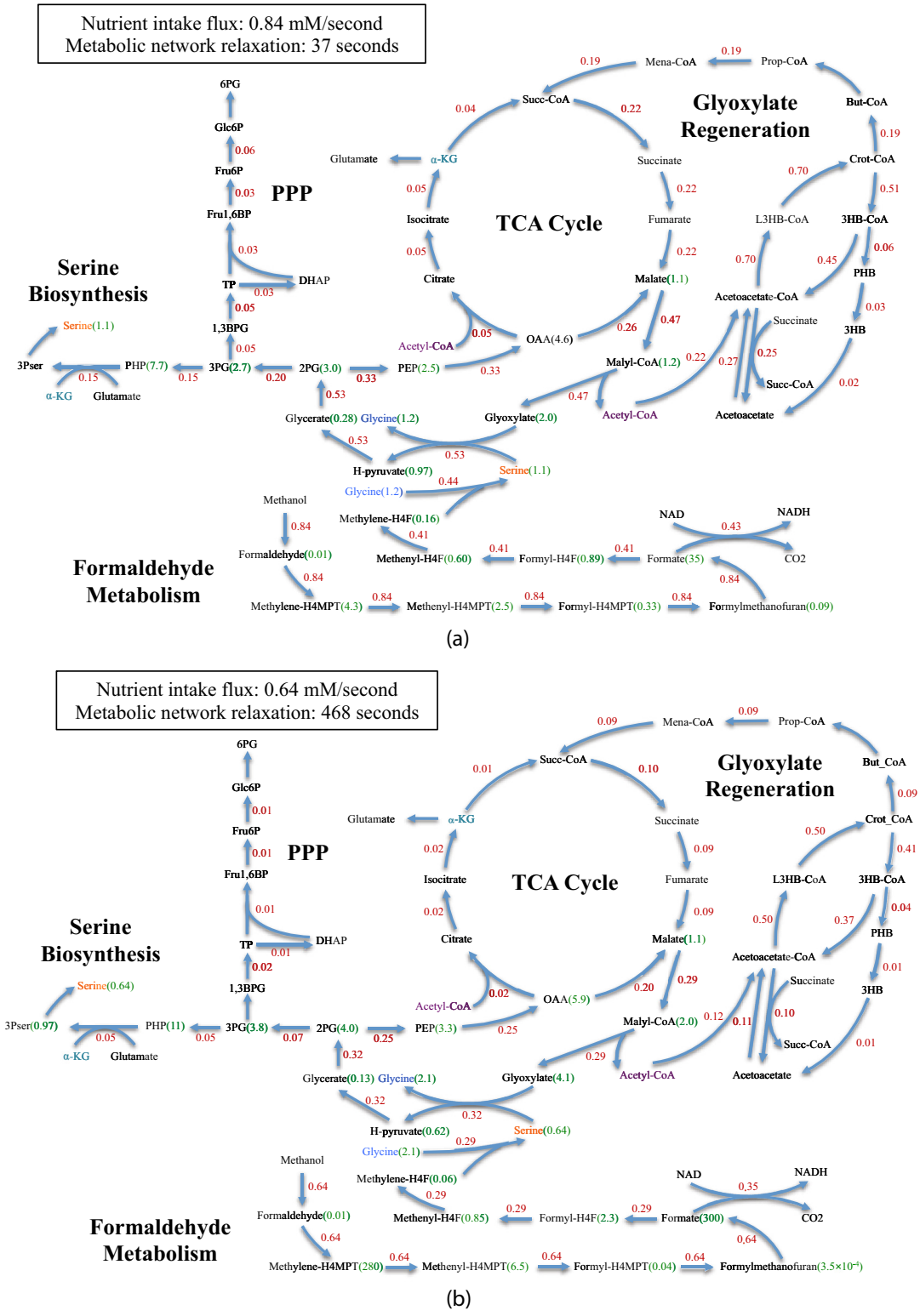

FIG. 3. Calculated steady-state fluxes in the dynamical model for *Methylobacterium extorquens* AM1 using two different sets of initial values. See Supplemental Material [43] for detailed results, in the excel files. The set of parameters supporting a stable metabolic network is not unique. However, the dynamical performance for the network with different parameters can be evaluated and compared with experiments. The more efficient network (b), i.e., with less carbon intake on the set biomass output, is less viable due to a larger relaxation time and a wider spread of metabolite concentrations. It also has less fluxes wasted in futile cycles. The fluxes given in (a) agree well with experiments. The fluxes are in red; the unit is mM/second. The concentrations of selected metabolites are in green; the unit is mM. Note that some fluxes are combination of multiple reactions and some fluxes and reactions are not shown in the figure.

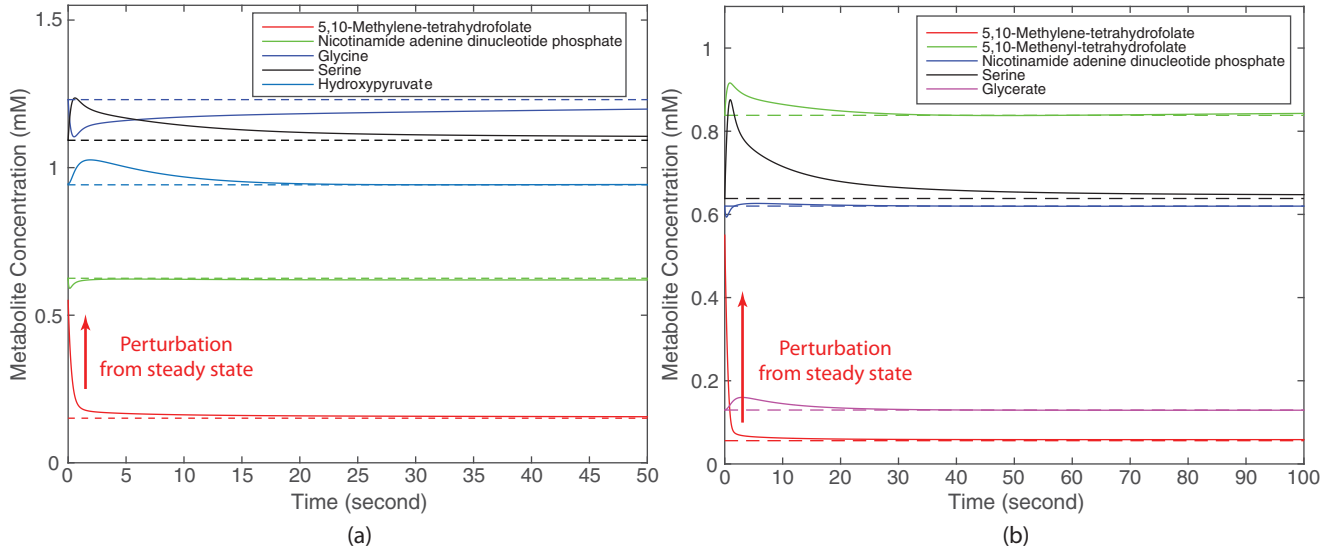

FIG. 4. Time-dependent relaxation of metabolites when perturbed from their steady-state values are shown in (a) and (b), calculated from parameters corresponding to Figs. 3(a) and 3(b). It confirms that the parameters in Fig. 3(b) indeed results in a longer relaxation time.

the organism can all be studied. Our construction is built upon a previously developed stochastic decomposition, the latter offers a potential landscape via a Lyapunov function on the network [26,38,44]. The regulatory dynamics can be simplified in the biochemical context for practical purposes. Moreover, as network stability is a generic topic in many fields, our work might have implications beyond a simple mathematical method for establishing kinetic metabolic models [45–47].

Biologically, we aim to provide a useful tool to analyze and extract properties of large metabolic networks whose parameters are difficult to obtain from *in vivo* measurements. Our approach differs from the usual type of methods that are based on static stoichiometric matrices plus conservations and/or optimizations. Our results offer a range of kinetic metabolic models (solutions) all having stable steady states under which dynamical metabolic properties can be analyzed. One such property is the relaxation time of a steady state, the inverse of which can be interpreted as the viability of a cell. It allows us to quantify the tradeoff between the growth efficiency (on carbon conversion rate) and the viability (as inverse of the relaxation time, futile cycles) of an organism. Hence we can sift through the solutions to identify the most appropriate one under a given physiological condition. Finally, large scale metabolic modeling may also offer global perspective on metabolic engineering [48].

ACKNOWLEDGMENTS

The work was partially supported by the Natural Science Foundation of China No. 91329301 and No. 91529306 (PA), No. 81273404 and No. 81473105 (MJX). We thank Prof. A. J. Leggett for many insightful discussions during his visits to Shanghai Jiao Tong University. One of us (Y.-C. Chen) is grateful for the hospitality of Shanghai Center for Systems Biomedicine during his visits.

APPENDIX: GENERIC RATE EQUATION FROM ORDERED UNI-BI MECHANISM

We can explicitly derive the generic rate equation in the ordered Uni-Bi mechanism as a demonstration [32]. The ordered Uni-Bi mechanism is schematically shown in Fig. 5. There are two products P and Q [34]. The final steady-state rate equation for the ordered Uni-Bi mechanism, when the intermediate enzyme states are eliminated, is given by [34]

$$u = \frac{N_1 A - N_2 P Q}{D_1 + D_2 A + D_3 P + D_4 Q + D_5 A P + D_6 P Q} \tag{A1}$$

under quasi-steady-states assumption. Here A and P, Q are the concentrations of the substrate and products in the reaction. The eight quantities N_1, N_2, and D_1–D_6 are functions of the six rate constants $\nu_{\pm 1}$, $\nu_{\pm 2}$, $\nu_{\pm 3}$ as well as the enzyme concentration e_0:

$$N_1 = \nu_1 \nu_2 \nu_3 e_0,$$
$$N_2 = \nu_{-1} \nu_{-2} \nu_{-3} e_0,$$
$$D_1 = \nu_2 \nu_3 + \nu_{-1} \nu_3,$$
$$D_2 = \nu_1 \nu_2 + \nu_1 \nu_3,$$

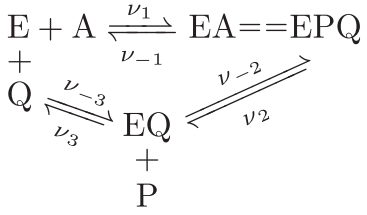

FIG. 5. Ordered Uni-Bi mechanism.

$$D_3 = \nu_{-1}\nu_{-2},$$
$$D_4 = \nu_{-3}\nu_2 + \nu_{-3}\nu_{-1},$$
$$D_5 = \nu_1\nu_{-2},$$
$$D_6 = \nu_{-2}\nu_{-3}.$$

The numerator in Eq. (A1) can be rewritten as

$$A\underbrace{(N_1/D_1)}_{V_F/K_A} - PQ\underbrace{(N_2/D_1)}_{V_B/K'_PK'_Q} = V_F\frac{A}{K_A} - V_B\frac{PQ}{K'_PK'_Q},$$

where the underbraces indicate that N_1/D_1 has been rewritten into V_F/K_A and likewise for the other term. After dividing by D_1, the denominator of Eq. (A1) becomes

$$1 + D'_2A + D'_3P + D'_4Q + D'_5AP + D'_6PQ, \qquad \text{(A2)}$$

where $D'_2 = D_2/D_1 \ldots D'_6 = D_6/D_1$. Defining $f_1 + f_2 = 1$ and regrouping Eq. (A2), we have

$$\begin{aligned}
1 + D'_2A + D'_3P + D'_4Q + D'_5AP + D'_6PQ &= f_1 + D'_2A + f_2 + P\underbrace{(D'_3 + D'_5A)}_{D''_3} + D'_4Q + D'_6PQ \\
&= f_1\left[1 + A\underbrace{(D'_2/f_1)}_{1/K_A}\right] + f_2\left[1 + P\underbrace{D''_3/f_2}_{g} + Q\underbrace{(D'_4/f_2)}_{h} + PQ\underbrace{(D'_6/f_2)}_{l}\right] \\
&= f_1(1 + A/K_A) + f_2(1 + P(g + Ql\alpha) + Q(h + Pl\beta) + PQl(1 - \alpha - \beta)) \\
&= f_1(1 + A/K_A) + f_2\left[1 + P\underbrace{(g + Ql\alpha)}_{1/K'_P}\right]\left[1 + Q\underbrace{(h + Pl\beta)}_{1/K'_Q}\right] \\
&= f_1\left(1 + \frac{A}{K_A}\right) + f_2\left(1 + \frac{P}{K'_P}\right)\left(1 + \frac{Q}{K'_Q}\right).
\end{aligned}$$

In the above we have defined $D''_3 = D'_3 + D'_5A$, $1/K_A = D'_2/f1$, $g = D''_3/f2$, $h = D'_4/f2$, $l = D'_6/f_2$, $1/K'_P = g + Ql\alpha$, and $1/K'_Q = h + Pl\beta$. K'_P and K'_Q are defined if $(g + Ql\alpha)(h + Pl\beta) = l(1 - \alpha - \beta)$, the latter should be regarded as the equation for α and β. Since A, P, and Q are positive and so are all the D_i, g, h, and l must be positive. As a result, the sign of the term $Pl\beta$ follows the sign of β. Similarly, the sign of the term $Ql\alpha$ follows the sign of α. If $gh = l$, $\alpha = \beta = 0$. If $gh < l$, then a solution exists with $\alpha > 0$ and $\beta > 0$. If $gh > l$, there is a solution with $\alpha < 0$ and $\beta < 0$ [but $(g + Ql\alpha) > 0$ hence $(h + Pl\beta) > 0$]. To this end we have successfully transformed the reaction rate Eq. (A1) into the form of Eq. (4) in the sense that all the parameters defined in the latter are positive. Since Eq. (A2) does not have the exact polynomial expression as the denominator in Eq. (4), our derivation reveals the implicit approximation when regarding the apparent Michaelis-Menten constants as constant. Strictly speaking, they can partially depend on the concentrations.

[1] T. Shlomi, M. N. Cabili, and E. Ruppin, Mol. Syst. Biol. **5** (2009).
[2] E. Nevoigt, Microbiol. Mol. Biol. Rev. **72**, 379 (2008).
[3] E. Meléndez-Hevia, T. G. Waddell, R. Heinrich, and F. Montero, Eur. J. Biochem. **244**, 527 (1997).
[4] M. Koutinas, A. Kiparissides, E. N. Pistikopoulos, and A. Mantalaris, Comput. Struct. Biotechnol. J. **3**, 1 (2012).
[5] Z. P. Gerdtzen, in *Genomics and Systems Biology of Mammalian Cell Culture* (Springer, Berlin, 2012), pp. 71–108.
[6] U. Sauer, Mol. Syst. Biol. **2** (2006).
[7] C. H. Schilling, S. Schuster, B. O. Palsson, and R. Heinrich, Biotechnol. Progr. **15**, 296 (1999).
[8] M. Oldiges, M. Kunze, D. Degenring, G. Sprenger, and R. Takors, Biotechnol. Progr. **20**, 1623 (2004).
[9] U. Theobald, W. Mailinger, M. Baltes, M. Rizzi, and M. Reuss, Biotechnol. Bioeng. **55**, 305 (1997).
[10] G. Teschl, *Ordinary Differential Equations and Dynamical Systems*, Vol. 140 (American Mathematical Society, Philadelphia, 2012).
[11] Y. Tohsato, K. Ikuta, A. Shionoya, Y. Mazaki, and M. Ito, Gene **518**, 84 (2013).
[12] K. Peskov, E. Mogilevskaya, and O. Demin, FEBS J. **279**, 3374 (2012).
[13] A. Calderwood, R. J. Morris, and S. Kopriva, Front. Plant Sci. **5**, 646 (2014).
[14] A. Khodayari, A. R. Zomorrodi, J. C. Liao, and C. D. Maranas, Metab. Eng. **25**, 50 (2014).
[15] G. Jia, G. Stephanopoulos, and R. Gunawan, Metabolites **2**, 891 (2012).
[16] N. J. Stanford, T. Lubitz, K. Smallbone, E. Klipp, P. Mendes, and W. Liebermeister, PLoS One **8**, e79195 (2013).
[17] N. Jamshidi and B. Ø. Palsson, Biophys. J. **98**, 175 (2010).
[18] J. Zanghellini, D. E. Ruckerbauer, M. Hanscho, and C. Jungreuthmayer, Biotechnol. J. **8**, 1009 (2013).
[19] A. Flamholz, E. Noor, A. Bar-Even, W. Liebermeister, and R. Milo, Proc. Natl. Acad. Sci. USA **110**, 10039 (2013).
[20] Y. Toya and H. Shimizu, Biotechnol. Adv. **31**, 818 (2013).
[21] T. Fuhrer, E. Fischer, and U. Sauer, J. Bacteriol. **187**, 1581 (2005).

[22] A. Bar-Even, A. Flamholz, E. Noor, and R. Milo, Nat. Chem. Biol. **8**, 509 (2012).
[23] A. Berger, K. Dohnt, P. Tielen, D. Jahn, J. Becker, and C. Wittmann, PLoS One **9**, e88368 (2014).
[24] O. Kotte, B. Volkmer, J. L. Radzikowski, and M. Heinemann, Mol. Syst. Biol. **10**, 736 (2014).
[25] S. Danø, P. G. Sørensen, and F. Hynne, Nature **402**, 320 (1999).
[26] P. Ao, J. Phys. A: Math. Gen. **37**, L25 (2004).
[27] R.-S. Yuan and P. Ao, J. Stat. Mech. **2012**, P07010 (2012).
[28] Y. Ma, Q. Tan, R. Yuan, B. Yuan, and P. Ao, Int. J. Bifurcat. Chaos **24**, 1450015 (2014).
[29] R. Yuan, X. Wang, Y. Ma, B. Yuan, and P. Ao, Phys. Rev. E **87**, 062109 (2013).
[30] J. M. Berg, J. L. Tymoczko, and L. Stryer, *Biochemistry*, 5th ed. (W.H. Freeman, New York, 2002).
[31] L. Lee, L. Yin, X. Zhu, and P. Ao, J. Biol. Syst. **15**, 495 (2007).
[32] M. Xu, X. Zhu, P. Lin, and P. Ao, Prog. Biochem. Biophys. **38**, 759 (2011).
[33] W. Liebermeister, J. Uhlendorf, and E. Klipp, Bioinformatics **26**, 1528 (2010).
[34] I. H. Segel, *Enzyme Kinetics* (John Wiley & Sons, New York, 1975).
[35] H. F. Lodish, A. Berk, S. L. Zipursky, P. Matsudaira, D. Baltimore, J. Darnell *et al.*, *Molecular Cell Biology*, Vol. 4 (Citeseer, Princeton, NJ, 2000).
[36] C. Kwon, P. Ao, and D. J. Thouless, Proc. Natl. Acad. Sci. USA **102**, 13029 (2005).
[37] Y. Tang, R. Yuan, and Y. Ma, Phys. Rev. E **87**, 012708 (2013).
[38] Y. Ruo-Shi, M. Yi-An, Y. Bo, and A. Ping, Chin. Phys. B **23**, 010505 (2014).
[39] D. T. Gillespie, J. Chem. Phys. **113**, 297 (2000).
[40] X. Lei, W. Tian, H. Zhu, T. Chen, and P. Ao, Sci. Rep. **5**, 13597 (2015).
[41] L. Chistoserdova, S.-W. Chen, A. Lapidus, and M. E. Lidstrom, J. Bacteriol. **185**, 2980 (2003).
[42] P. Ao, L. W. Lee, M. E. Lidstrom, L. Yin, and X. Zhu, Chin. J. Biotechnol. **24**, 980 (2008).
[43] See Supplemental Material at http://link.aps.org/supplemental/10.1103/PhysRevE.93.062409 for additional information concerning the model and data used in the present study.
[44] L. Yin and P. Ao, J. Phys. A: Math. Gen. **39**, 8593 (2006).
[45] M. Ellis, H. Durand, and P. D. Christofides, J. Process Contr. **24**, 1156 (2014).
[46] P. Kokotović and M. Arcak, Automatica **37**, 637 (2001).
[47] S. Sastry, *Nonlinear Systems: Analysis, Stability, and Control*, Vol. 10 (Springer, New York, 1999).
[48] M.-J. Xu, Y.-C. Chen, P. Ao, and X.-M. Zhu, IET Systems Biology **10**, 17 (2016).